Desalination and Water Treatment
www.deswater.com

doi: 10.1080/19443994.2016.1171169

57 (2016) 26414–26426
November

Taylor & Francis
Taylor & Francis Group

Influence of palm oil fuel ash, an agro-industry waste on the ultrafiltration performance of cellulose acetate butyrate membrane

Seema S. Shenvi[a], Arun M. Isloor[a,*], Abdul Latif Ahmad[b], B. Garudachari[a], Ahmad F. Ismail[c]

[a]*Membrane Technology Laboratory, Department of Chemistry, National Institute of Technology Karnataka, Surathkal, 575 025 Mangalore, India, Fax: +91 824 2474033; email: isloor@yahoo.com (A.M. Isloor)*
[b]*School of Chemical Engineering, Universiti Sains Malaysia, USM Engineering Campus, Seri Ampangan, Nibong Tebal, Pulau Pinang 14300, Malaysia*
[c]*Advanced Membrane Technology Research Center (AMTEC), Universiti Teknologi Malaysia, 81310 Skudai, Johor Bahru, Malaysia*

Received 22 November 2015; Accepted 2 March 2016

ABSTRACT

Palm oil fuel ash (POFA), which is produced as waste during production of palm oil, was used as an alternative additive to prepare cellulose acetate butyrate (CAB) composite ultrafiltration membrane. Acid-activated-milled POFA was characterized by Brunauere–Emmette–Teller (BET) surface area analysis and infrared spectroscopy (IR). The effect of incorporation of POFA in CAB matrix was analyzed by contact angle, water uptake, and porosity studies. The studies revealed an enhancement in the hydrophilic nature of the composite membranes upon addition of POFA. The change in the morphology of the membranes was recorded by means of scanning electron microscopy (SEM) which revealed the changing asymmetric structure of the membrane. Pure water flux and antifouling studies indicated that the membranes exhibited enhanced flux recovery ratio, which was maximum for CAB 2 (87.6%) containing 2 wt.% of POFA. The adsorption property of POFA in addition to CAB/POFA network helped in the humic acid removal from aqueous solution up to 86% for CAB 2.5 membrane.

Keywords: Agrowaste; Ultrafiltration; Humic acid; Flux recovery ratio

1. Introduction

A number of pollutants, such as pesticides, textile dyes, heavy metals, humic substances, petrochemical compounds, and other industrial/municipal waste, are known to cause severe water contamination. Membrane technology for separation and water purification has already gained wide momentum due to its ease of operation in comparison with conventional techniques. With the growing emphasis on environmental conservation, usage of environmentally benign materials to make the entire membrane separation process economically and ecologically viable is imperative.

Cellulose is the most abundantly occurring biopolymer that has several advantages to offer as a membrane material [1]. However, the wide-scale utilization of cellulose is hindered due to its insolubility in most of the known solvents and its low processability. These shortcomings are overcome by the esterification of cellulose, which improves the solubility and

*Corresponding author.

processability of the material. Cellulose acetate butyrate (CAB), commonly known as CAB is one such derivative of cellulose, which is formed by the reaction of cellulose with acetic acid and butyric acid. It is known for its high glass transition temperature and good mechanical properties [2]. It is a thermoplastic material that offers good tolerance toward chlorine and has good chemical stability with good resistance toward fouling when used as membrane material in water treatment applications [3,4]. In comparison with cellulose acetate that is the most popular cellulose derivative, research on CAB is still an area to be explored extensively.

In the current work, palm oil fuel ash (POFA) was used as an additive to improve the performance of CAB membrane. Ash is generally obtained by the combustion of agricultural solid waste. Malaysia is one of the major exporters of palm oil and other palm tree-derived materials. During the extraction of palm oil, considerable amount of solid waste in the form of fruit bunches, fibers and nutshells are generated. This waste is reused in the palm oil milling industry in the form of fuel for the production of steam to generate electricity, leaving behind 5% ash (POFA) [5,6]. The ash thus generated poses environmental hazards when discharged in huge amounts in wastelands [7]. POFA contains large number of inorganic oxides, such as SiO_2, Al_2O_3, CaO, and Fe_2O_3, that are potential adsorption sites for the removal of various pollutants [8]. Additional physical properties of these oxides include high porosity, high particle size distribution, and high surface area [9,10]. Successful attempts have been made in the past to utilize agroindustrial waste for water treatment. The use of such industrial wastes, which are potential environment pollutants to curb water contamination, is an attractive notion that is leading to a new revolution in the field of membrane fabrication process [11–13]. Use of bagasse fly ash, rice husk ash, and fly ash have been reported to remove pollutants, such as metal ions, phosphorous, textile dyes, and phenols [14–21]. POFA has been used as an adsorbent in the past for the quantitative removal of chromium, reactive blue dye, and cadmium [22,23]. The possible use of this waste as an inorganic filler in the membrane matrix has not been explored so far to the best of our knowledge.

Humic acid (HA) is the main component of humic substances that are produced by the biodegradation of dead organic matter. In addition to imparting odor and color to water, HA is capable of reacting with chlorine in water to produce trihalomethanes that are potential carcinogenic agents [24,25]. Also, the existence of carboxylic and phenolic groups in HA may lead to changes in structural and chemical properties of HA depending upon different water environments. Hence, the removal of HA from water is one of the important measures that needs to be undertaken in water treatment. Polyaniline, aminated polyacrylonitrile, graphene oxide, gallic acid, and unburned carbon has been used in the past to remove HA [24,26–29]. However, the use of POFA as an additive to prepare UF membrane capable of improving the fouling resistance and removal of HA has not been investigated yet as per our knowledge.

The aim of the current work was to carry out a detailed investigation of the UF performance of CAB membranes using POFA as an additive. The membranes were subjected to different permeation tests to study the pure water flux (PWF), antifouling property, flux recovery ratio (FRR), and HA removal.

2. Experimental

2.1. Materials

CAB (M_w ~65 kDa, butyryl content 16.5–19.0%, acetyl content 28–31%) was procured from Himedia, Mumbai. POFA was obtained from United Palm Oil Industries, Nebong Tebal, Malaysia. *N*-Methyl pyrrolidone (NMP) of analytical grade was supplied by Merck, India and was used without further purification. Bovine serum albumin (BSA) (M_w ~69 kDa) used for antifouling study was procured from CDH chemicals. HA received from Himedia was dissolved in water whose pH was maintained at 8.4 using $NaHCO_3$ buffer solution. The solution was kept for stirring overnight after which it was centrifuged to remove the undissolved solid matter. The clear supernatant solution of HA was further used for analysis.

2.2. Pretreatment of POFA

The as such received POFA from oil mill was first subjected to mechanical sieving to obtain particle size less than 45 μm. It was then thoroughly washed with distilled water for 4–5 times to remove other suspended particles from the supernatant solution of POFA. It was dried for 48 h in an oven at 80°C. Dry POFA was further ball milled (Retsch MM200) for 5 h to obtain particle size up to 20 μm. The ash was activated by 1 M HCl solution under refluxing conditions for 4 h after which the solution was filtered and the residue was repeatedly washed with distilled water until filtrate was neutral. It was finally dried overnight in the oven before subjecting it to further analysis [23].

2.3. Preparation of CAB/POFA composite membrane

First, the pretreated POFA was dispersed in NMP solvent for 2 h after which it was ultra sonicated for

15 min to ensure uniform dispersion. CAB (12.5 wt.%) was then added to the above solution and kept for stirring for 24 h. After ensuring polymer dissolution, the casting solution was degassed to get rid of trapped air bubbles. The composite membranes were cast on a glass plate with the aid of an automated membrane casting machine. The glass plate with nascent membrane was initially kept for 30 s in air for evaporation before dipping it in coagulation bath for phase inversion [30]. The film separated from glass plate after the completion of phase inversion process. Composition of the composite blends is as mentioned in Table 1.

3. Characterization of POFA and composite membranes

3.1. Analysis of pretreated POFA

Brunauere–Emmette–Teller (BET) surface area analysis and porosity measurements of POFA were carried out on Micrometrics ASAP 2020 model. The particle size analysis of the milled POFA was analyzed on CIS-50 ANKERSMID. The chemical constitution of POFA was characterized by recording the infrared (IR) spectrum on JASCO 4200. The spectra were recorded in the working range 600–4,000 cm^{-1}.

3.2. Contact angle measurement of composite membranes

To verify the change in surface hydrophilicity of the prepared membranes by the addition of POFA, contact angle was recorded on FTA-200 dynamic contact angle analyzer. The instrument recorded the angle formed by the water droplet with the membrane surface. In this study, a water droplet was carefully deposited on the surface of the membrane with the aid of microsyringe, and the contact angle was measured until no further change was observed [31].

Table 1
Composition of CAB/POFA composite membranes

	Polymer concentration (wt.%)		
Membrane code	CAB	POFA	Solvent (wt.%)
CAB 0	12.5	–	87.5
CAB 1	12.5	1	86.5
CAB 1.5	12.5	1.5	85.5
CAB 2	12.5	2	84.5
CAB 2.5	12.5	2.5	83.5

3.3. Water uptake and porosity measurements

Water uptake capacity of the membranes was calculated using the following formula:

$$\%\ \text{Water content} = \left(\frac{W_w - W_d}{W_w}\right) \times 100 \quad (1)$$

where W_w and W_d are the weight of wet and dry membrane samples respectively. Porosity of the composite membrane was carried out as mentioned in the literature by Chen et al. [32]. Membrane samples sized 1 cm^2 were immersed in distilled water for 24 h. The weight of the wet membrane was noted as M_w after carefully blotting the surface adhering water by filter paper. It was then dried till constant mass was obtained as M_d. From M_w and M_d, porosity was calculated as:

$$\varepsilon\ (\%) = \frac{M_w - M_d}{A \times l \times \rho} \times 100 \quad (2)$$

where A is the area of the sample (cm^2), l is the thickness (cm) and ρ is the density of water (0.998 g/cm^3).

3.4. Morphology study of the composite membranes

CAB/POFA composite membranes were subjected to different characterization. The surface and cross sectional morphology of the membranes in addition to elemental mapping and energy-dispersive X-ray (EDX) analysis was investigated through scanning electron microscopy (SEM). The SEM images were recorded on Jeol JSM-6380LA after the samples were cryogenically fractured by dipping in liquid nitrogen for 1 min.

3.5. Permeation study of the composite membrane

The permeation properties of the membranes were studied on laboratory-fabricated UF kit, having a membrane holder of effective diameter of 5 cm. The membranes were subjected to compaction at 0.45 MPa pressure for 1 h. The permeation studies were carried out on membranes at room temperature and at 0.4 MPa. The PWF was calculated as:

$$J_w = \frac{Q}{A \times t} \quad (3)$$

where J_w (L/m^2 h) is the PWF, Q is the volume of water (L) permeated through the membrane of area A (m^2) in time t (h). The antifouling property was studied using 1,000 mg/L of BSA solution. The experiment was carried out in three cycles; firstly, PWF J_{w1} was determined followed by protein flux J_p. After BSA

filtration, the feed solution in the tank was replaced by distilled water and the membrane coupon was flushed with water to remove loosely adhering BSA molecules. PWF of thus cleaned membrane was recorded as J_{w2}. FRR was calculated from these values to evaluate the antifouling performance of the membrane as follows:

$$\text{FRR } (\%) = \frac{J_{w2}}{J_{w1}} \times 100 \tag{4}$$

The resistance offered by the membrane is an indication of the extent of membrane fouling that was calculated in terms of total fouling as follows:

$$R_t \ (\%) = \left(1 - \frac{J_p}{J_{w1}}\right) \times 100 \tag{5}$$

where R_t is the flux loss due to total fouling that was the sum of reversible (R_{rev}) and irreversible fouling ratio (R_{irr}) [33,34].

$$R_t = R_{rev} + R_{irr} \tag{6}$$

$$R_{rev} \ (\%) = \frac{(J_{w2} - J_p)}{J_{w1}} \times 100 \tag{7}$$

$$R_{irr} \ (\%) = \left(\frac{J_{w1} - J_{w2}}{J_{w1}}\right) \times 100 \tag{8}$$

The permeation experiments were carried out in duplicate and their average value was reported.

In addition to this, 100 mg/L of HA solution was used as feed to study the rejection performance of the composite membrane. The concentration of HA in the feed and permeate solutions was recorded on ultraviolet-visible (UV–vis) spectrophotometer (Analytikjena Specord S600) at 254 nm. HA rejection was calculated as follows:

$$R \ (\%) = \left(1 - \frac{C_p}{C_f}\right) \tag{9}$$

where C_p and C_f is concentration of HA in permeate and feed solution respectively.

4. Results and discussion

4.1. Characterization of POFA

The particle size distribution of milled POFA is shown in Fig. 1. It is observed from the figure that the mean value of the particles is ~13 μm with a standard deviation of 6.25. The graph exhibited a bimodal nature, indicating the particle size distribution of POFA was not uniform. The size of some POFA particles was observed to be less than 2 μm.

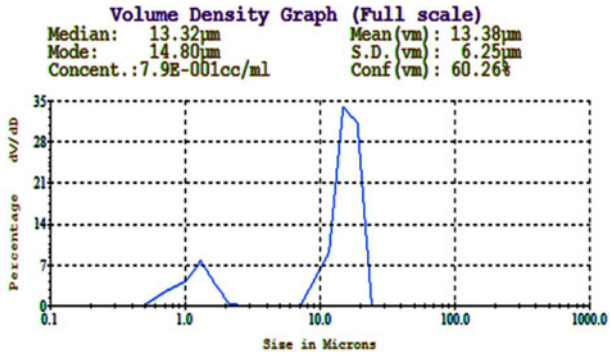

Fig. 1. Particle size distribution of milled POFA.

Sieved particles of 45 μm when used in the preparation of composite membranes were observed to settle down in the casting solution. This in turn resulted in the nonuniform dispersion of POFA in the polymer matrix. This problem was overcome and homogeneity was achieved when particle size was reduced by milling.

The chemical composition of POFA mainly comprises SiO_2 ranging from 44 to 66% and Al_2O_3 in the range 1.5–11.5% [5,35]. It also includes other components such as Fe_2O_3 and CaO. The BET analysis results have been summarized in Table 2. Surface area measuring 11.79 m^2/g indicated the adsorption property of milled POFA which bestowed it with the capacity to adsorb contaminants including HA. Acid activation is reported to have improved the surface area of the ash [36,37].

The FTIR spectrum of POFA has been shown if Fig. 2. The figure exhibits a small broad band between 3,300 and 3,500 cm^{-1} which is attributed to both silanol groups (Si–OH) and adsorbed water on the surface [15,16,38]. Peaks at 1,105 cm^{-1} was assigned to Si–O–Si and Al–O stretch [39,40]. Peak at 667 cm^{-1} was due to Si–H present in POFA where as another peak due to Al–O stretch was observed at 786.85 cm^{-1}.

Table 2
BET surface area analysis of the activated POFA

BET surface area	11.7969 m^2/g
BJH adsorption average pore diameter	511.378 Å
BJH adsorption cumulative volume of pores	0.0069 cm^3/g

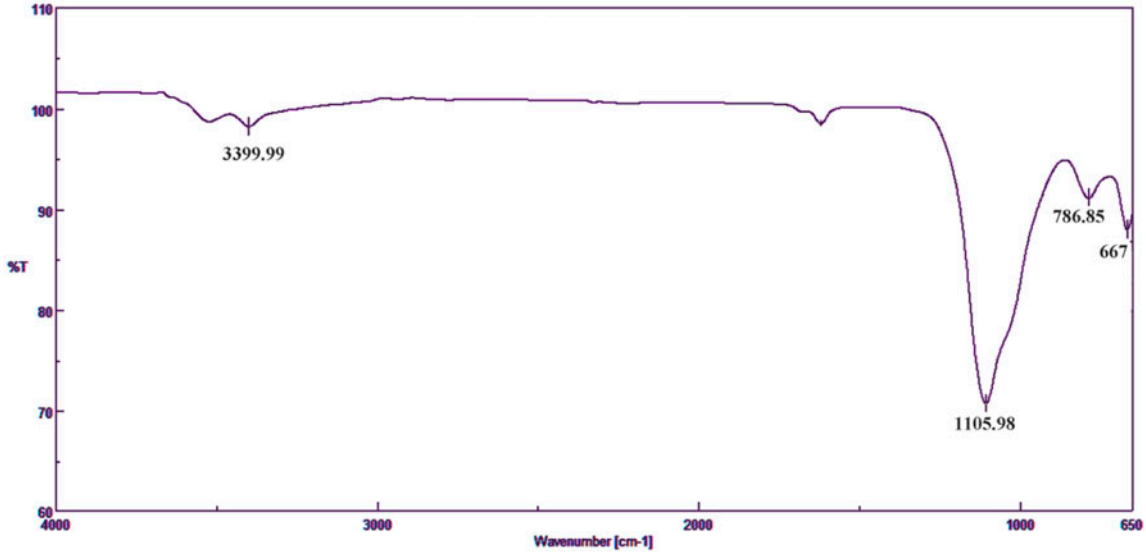

Fig. 2. FTIR spectrum of POFA.

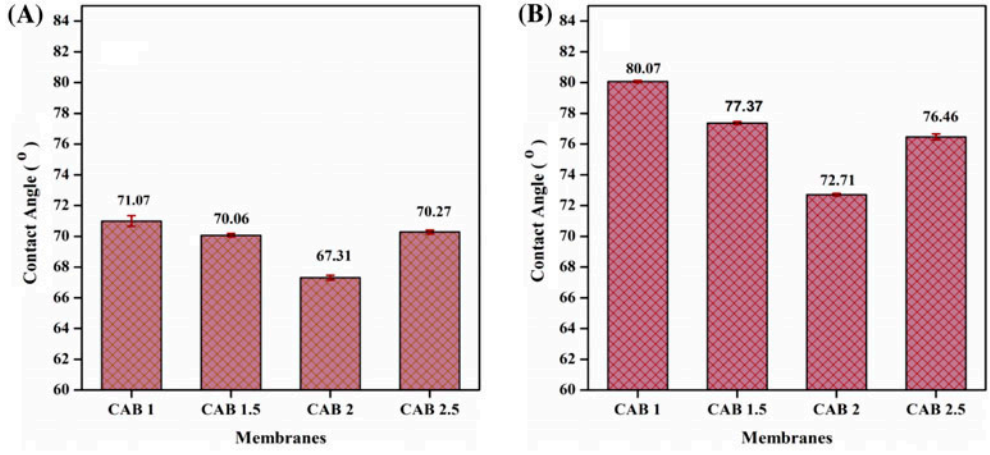

Fig. 3. Contact angle for (A) active surface of CAB/POFA and (B) rear surface of CAB/POFA.

4.2. Contact angle analysis

The change in the surface hydrophilicity by addition of POFA to CAB was investigated by means of recording the contact angle. The contact angle of the active surface of CAB 0 membrane was recorded to be 73.17°. However, with the addition of POFA in membrane matrix, the contact angle decreased, which indicated the changing nature of the membrane surface. The contact angle decreased from 71.07° for CAB 1 to 67.31° for CAB 2 after which the contact angle increased again as evidenced from Fig. 3(A). The increase in hydrophilicity may have been due to the migration of POFA to the top surface during phase inversion due to its affinity toward water. Such migration of hydrophilic additives to the top surface during phase inversion has been observed in literature too [41]. Movement of POFA particles to the top layer was further justified by the relatively high contact angle values of the rear surface (bottom) of composite membranes as shown in Fig. 3(B). During membrane formation, it was also observed that the active surface exhibited a deeper gray shade than the bottom layer that proves the above theory of POFA movement. The contact angle started increasing on further addition of POFA after 2 wt.%. This can be attributed to possible leaching of POFA in water bath during phase inversion due to increased thermodynamic instability within the polymer matrix with increment in the content of inorganic filler. The presence of less amount of

POFA on the top surface resulted in higher contact angle reflecting a reduction in membrane hydrophilicity after CAB 2. Another probable explanation for this trend is non-uniform distribution of POFA at higher concentration. Formation of POFA aggregates arising from steric hindrance and electrostatic interaction between CAB–POFA as well as among POFA particles affected its dispersion in the membrane matrix and on its surface [31,42].

4.3. Water uptake and porosity studies

The change in water uptake measurements after addition of POFA indicated an increase in bulk hydrophilicity of the membranes in the order CAB 2.5 > CAB 2 > CAB 1.5 > CAB 1 (Fig. 4(A)). The water uptake for neat CAB membrane was found to be 49.2%. Maximum water uptake of 75% was observed for CAB 2.5. Even though the surface hydrophilicity decreased in CAB 2.5 as discussed in the previous section, leaching of POFA from the composite membrane during phase inversion resulted in void formation giving rise to free volume (void) in membrane structure. This increased the water holding capacity of CAB 2.5 membrane that was reflected in the water uptake study.

POFA enhanced the porosity of the membranes up to 2 wt.% (Fig. 4(A)). Beyond this concentration, the

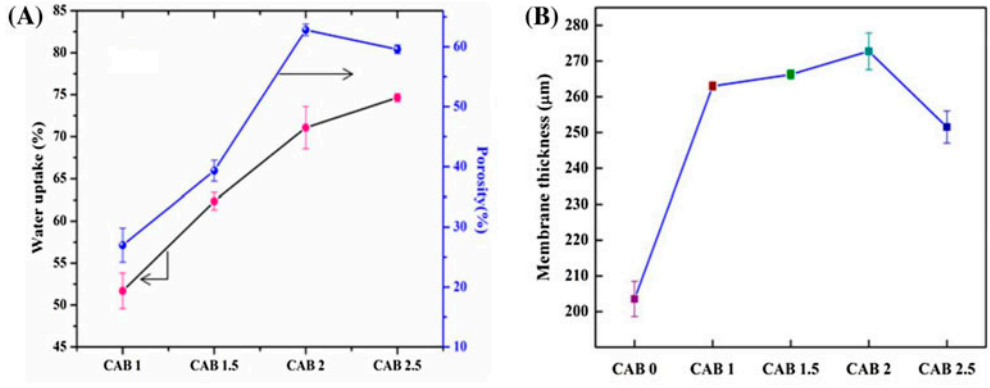

Fig. 4. (A) Water uptake and porosity measurements of composite membranes and (B) effect of variation in POFA on membrane thickness.

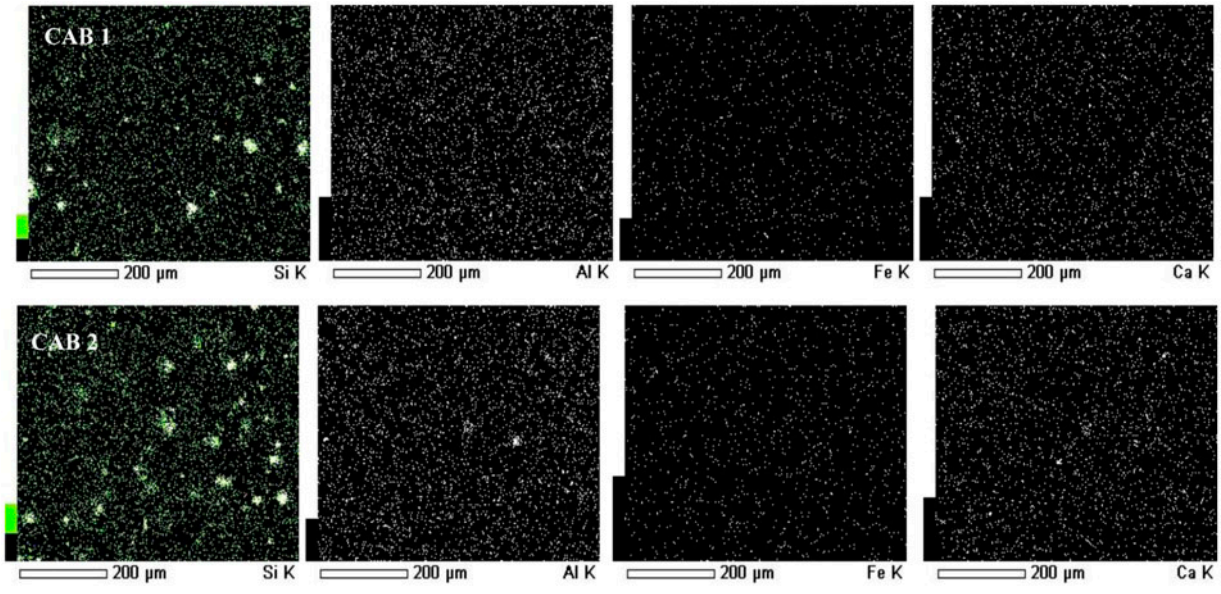

Fig. 5. Elemental mapping of the surface of CAB 1 and CAB 2.

porosity decreased from 62.13 to 59.08%. This observation must have been due to aggregartion and blocking of pores after CAB 2, which declined the connectivity between the pores. The effect of variation in POFA concentration was further correlated with the thickness of the composite membranes that affected its porosity. It was observed that (Fig. 4(B)), the membrane thickness increased with increase in concentration of POFA. However, this increase was perceived only up to 2 wt.%. Beyond 2 wt.%, the thickness decreased. This was in accordance with literature, where at higher concentration, the casting solution caused compaction and the membrane thickness decreased. Compaction led to denser structure and had a negative effect on porosity and permeability. This compaction factor along with substantial pore blockage was one of the primary reasons for the decrease in porosity and permeation at 2.5 wt.% POFA concentration. Moreover, above 2.5 wt.% uniform dispersion of POFA was affected due to aggregation in the increasingly viscous polymer solution [43,44]. The increased viscosity of the solution made it difficult to cast membranes. Owing to these reasons, the concentration of POFA was restricted to 2.5 wt.%.

4.4. Morphological analysis of composite membranes

Figs. 5–7 give a detailed account of the morphology and the elemental composition of POFA/CAB composite membranes. Elemental mapping of the sur-

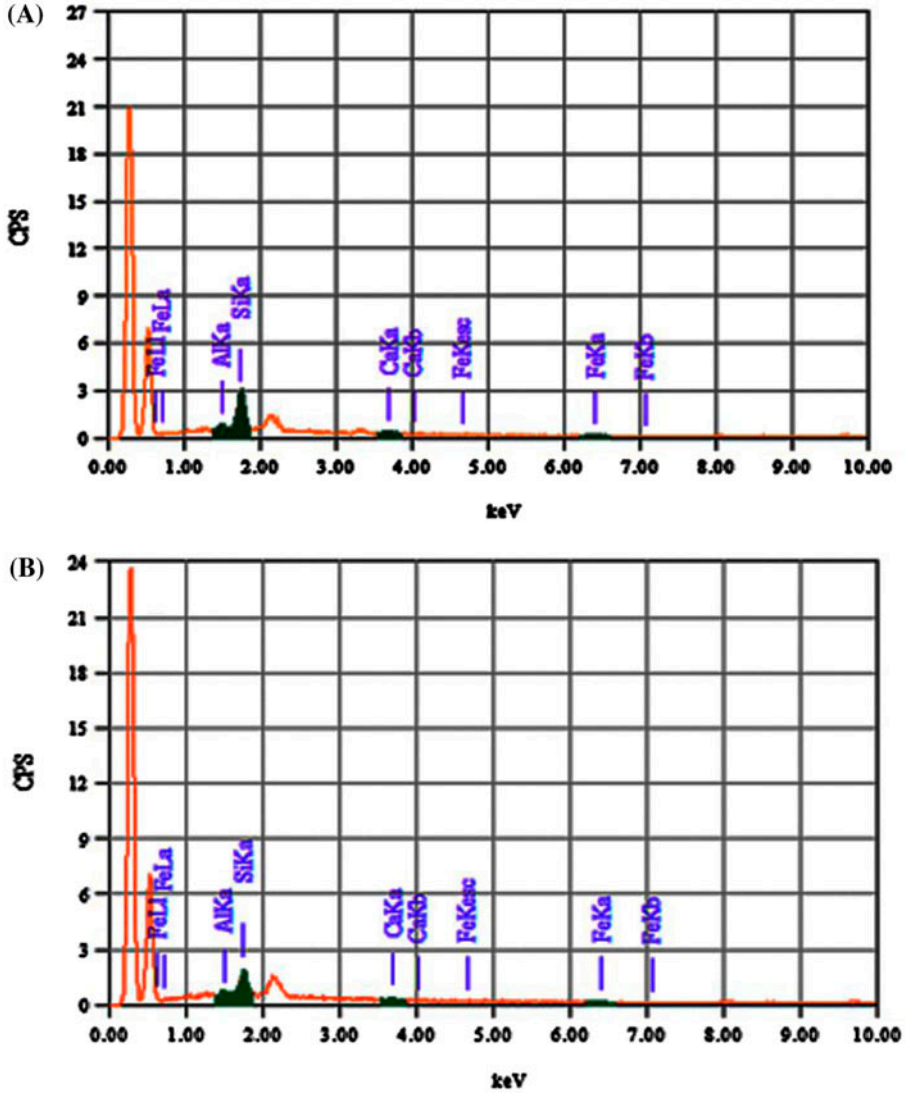

Fig. 6. EDX analysis of (A) CAB 1 and (B) CAB 2.

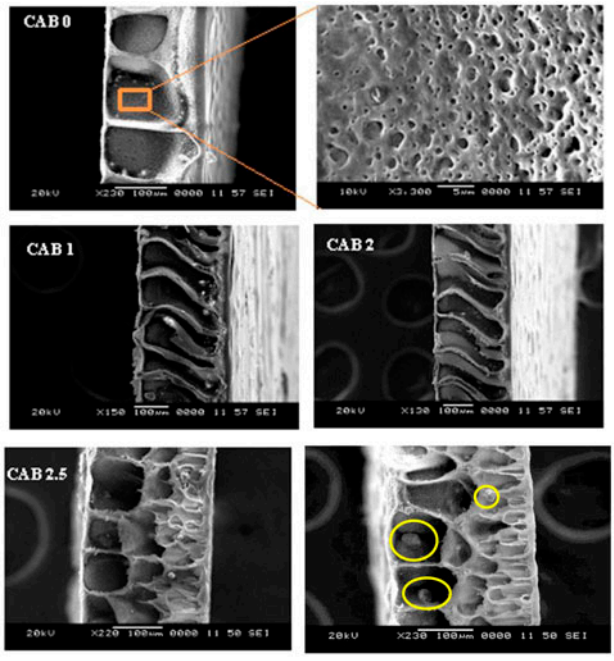

Fig. 7. Cross-section morphology of POFA/CAB composite membranes.

face of CAB 1 and CAB 2 is shown in Fig. 5. The content of SiO_2 being maximum in ash, elemental mapping for Si element was observed to be highest on the membrane surfaces. This was followed by Al, Ca and Fe. Ca and Fe content in the membrane were almost same. Moreover, in comparison with CAB 1, CAB 2 showed higher distribution of the elements, i.e. ash. This confirmed the increase in POFA loading in the membrane from CAB 1 to CAB 2. Fig. 5 also proves uniform distribution of POFA in the membrane matrix. Incorporation of POFA in the composite membranes was further proved by recording the EDX spectra (Fig. 6).

The cross section morphology of CAB 0 and the composite membranes is shown in Fig. 7. It was observed that all the membranes exhibited asymmetric nature with a thin dense skin layer followed by a porous sublayer. In case of CAB 0, a very open structure with a thin skin, followed by wide and large finger-like projections running down through the entire width of the membrane was observed. The walls of the finger like structures were too narrow. At higher magnification, it was seen that, CAB 0 had a very "loose" morphology, which was not very ideal for separation applications.

With the addition of POFA in CAB, the morphology changed slightly up to 2 wt.%. The membranes CAB 1 and CAB 2 still possessed finger-like morphology, however, with thinner skin and the projections were not as wide as that of CAB 0. The thinner active layer was due to instantaneous demixing during phase separation. When the percentage of POFA was increased to 2.5 wt.%, there was a drastic change in the morphology of the membrane. The membrane CAB 2.5 now showcased a thin layer, followed by not very well-defined finger-like projections that were ultimately followed by macrovoids. This observation can be explained on the basis of viscosity of the solution affecting the phase separation phenomenon. At higher percentage of POFA, the viscosity of casting solution increases, which has an influence on the kinetics of phase separation process. The formation of finger-like morphology and macrovoids is a direct result of phase separation kinetics. Instantaneous demixing of solvent and nonsolvent during phase inversion results in the formation of finger-like projections, whereas delayed phenomenon leads to the suppression of void formation [45]. The membrane formation process was slowed down to a considerable extent with increased viscosity, thus shifting the demixing progression from instantaneous to a delayed one. Increase in viscosity also hinders the free movement of additives that limits the formation of development of membrane pore structure. This in turn had a negative effect on the permeability of the membrane. Moreover, it was also observed that POFA particles partially blocked the open pores at higher concentration. The presence of POFA in the cross section of CAB 2.5 has been highlighted in Fig. 7.

4.5. Permeation studies

4.5.1. Antifouling study

PWF and FRR experiments on POFA/CAB composite membranes were carried out at 0.4 MPa

Table 3
Summary of permeation studies performed on POFA/CAB composite membranes

Membranes	PWF (L/m^2 h)	FRR (%)	HA removal (%)	Contact angle (°)	Porosity (%)	Water uptake (%)
CAB 1	126.89	32.1	49.4	71.07	21.03	53.19
CAB 1.5	113.11	48.12	58.21	70.06	36.57	61.64
CAB 2	90.087	87.64	74.39	67.31	62.13	72.86
CAB 2.5	25.97	72.1	85.78	70.27	59.08	75

pressure. BSA was chosen as the model protein foulant in this study. PWF of CAB 0 membrane was recorded to be 51.38 L/m^2 h. The PWF of all the composite membranes was higher than that of CAB 0 membrane (except CAB 2.5). This was attributed to increased porosity and well-structured morphology of the composite membranes. However, flux reduced drastically from 126 to 25.97 L/m^2 h from CAB 1 to CAB 2.5, respectively, (Table 3) with increase in POFA content. Even though there was increase in hydrophilicity, which was evidenced by contact angle, water uptake study and porosity, the PWF declined with increase in POFA concentration from 1 to 2.5 wt.%. The possible explanation for this behavior of composite membrane may be ascribed to the micron-sized POFA particles. Large-sized POFA particles resulted in a "tight" network and some dead-end pores. This meant that the membrane structure became more compact with reduced pore size as the POFA concentration increased in the membrane. Hence, maximum flux was observed for CAB 1 membrane containing least amount of POFA. Thus, other factors also tend to affect the linear relation between porosity and flux [46]. At higher concentration of POFA, i.e. for CAB 2.5, pore plugging phenomenon must have been very severe resulting in PWF value as low as 25 L/m^2 h. Also, the decreased porosity and changing morphology contributed to the drastic flux decline in CAB 2.5.

FRR reflects hydrophilicity and reusability of the membrane. While measuring the FRR of POFA/CAB composite membranes, it was observed that, with an increase in POFA concentration, FRR improved reasonably. This was attributed to the partial hydrophilic nature of the composite membranes due to incorporation of POFA in the membrane matrix. Detachment of BSA molecules became relatively easy due to the water adsorbed on the membrane surface having POFA [47]. FRR increased steadily from very low value of 32.1–87.64% from CAB 1 to CAB 2, respectively, which was in accordance with hydrophilicity of the membranes (Table 3). Beyond this, at 2.5 wt.%, the value decreased to 72.6%. This was due to reduced surface hydrophilicity for CAB 2.5.

The water and BSA flux behavior of composite membranes is shown in Fig. 8. From the sudden decline in flux value during BSA filtration, it was concluded that, fouling by BSA is initiated within first few seconds of filtration. Fouling proceeded by pore plugging and cake formation on membrane surface, thereby resulting in flux decline over a period of time [48]. The entire permeation study has been summarized in Table 3.

Fig. 9 shows total fouling ratio (R_t), reversible fouling (R_{rev}) and irreversible fouling (R_{irr}) values (%) for the prepared composite membranes. Reversible fouling arises from reversible foulant adsorption on membrane surface that can be conveniently removed by simple hydraulic cleaning. Irreversible fouling arises either by strong binding of foulants to the membrane surface or by trapping of foulant molecules in the membrane pores. Cleaning of such irreversibly fouled membranes is a tedious process requiring chemical treatment that increases the operating cost. Thus, in conclusion, higher the reversible fouling ratio, more economic is the membrane cleaning process. It was observed that, CAB 0 had the highest R_{irr} toward BSA, which was nearly 70% of the total fouling.

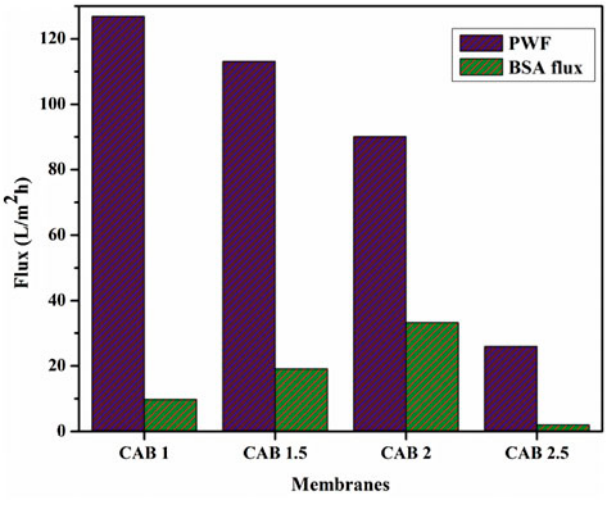

Fig. 8. Pure water and BSA flux of composite membranes.

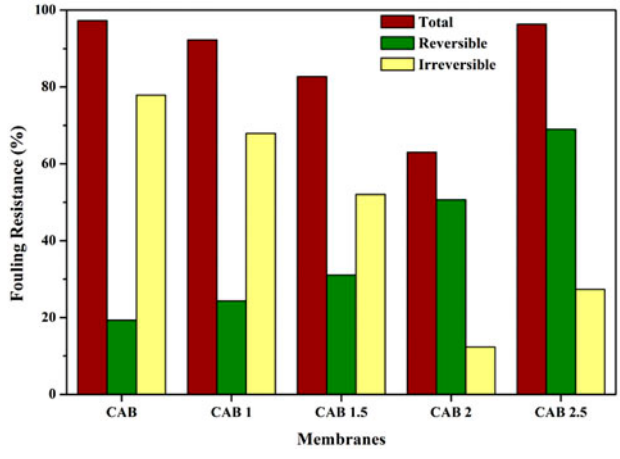

Fig. 9. Fouling resistances of CAB/POFA composite membranes.

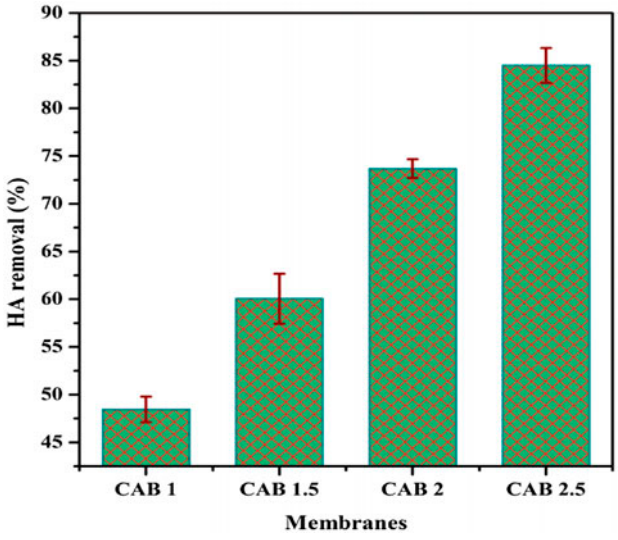

Fig. 10. Removal of HA by the composite membranes.

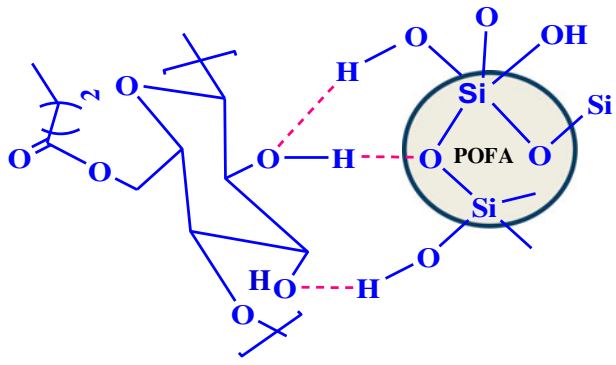

Fig. 11. Plausible interactions between CAB and POFA.

However, with the addition and increase in POFA from CAB 1 to CAB 2, the percentage of R_{irr} decreased, whereas that of R_{rev} increased. This was due to increase in the formation of protein-resistant hydrophilic membrane surface, which led to strong binding of water molecules making it difficult for protein molecules to adhere strongly to the membrane surface [49]. However, upon further addition of POFA, the membrane performance dipped sharply that must be due to decreased hydrophilicity and agglomeration of ash on the membrane surface.

4.5.2. HA removal

The prepared composite membranes were subjected to check HA removal. POFA possesses good adsorption capacity as realized from the BET surface area analysis. It was assumed that the adsorptive nature of POFA may assist in the removal of HA. The results obtained proved that POFA/CAB membranes indeed behaved as adsorption membranes. CAB 2.5 showed maximum rejection towards HA up to 85% (Fig. 10). Separation in adsorption membranes occurs both by size exclusion and by adsorption. HA may contain molecules ranging from few hundreds to thousand daltons. The compact network formed by CAB with POFA help retain the large HA molecules. The plausible interaction between CAB segments and POFA particles has been represented in Fig. 11. The hydroxyl group present on the surface of POFA is engaged in hydrogen bonding with CAB. Such interactions of polymer matrix with ash have been reported in literature [39,50]. In addition to this, the adsorption property of POFA also helps in retaining HA. This cohesive effect results in higher rejection of HA at higher POFA concentration. Also, the role of POFA in rejection of HA was confirmed by the fact that, CAB 0 did not show any HA removing capacity. Fig. 12(A) shows the surface image of HA fouled CAB 2.5 membrane. It is observed that the surface of the membrane became slightly brown with few HA molecules adsorbed on the membrane surface. The HA

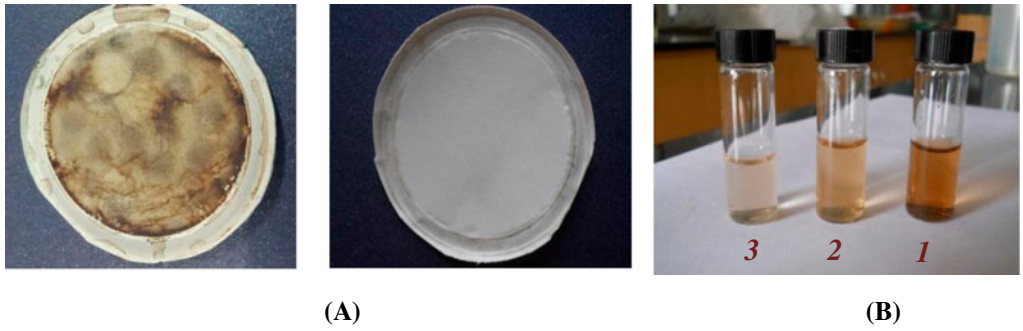

Fig. 12. Digital images of (A) HA fouled and unfouled membrane and (B) HA permeated through (1) CAB 0, (2) CAB 1.5 and (3) CAB 2.5.

Table 4
HA removal capacity of other commercial and reported UF membranes

Membrane	Additive	HA removal (%)	Refs.
UAM 300[a]	–	98	[51]
Amicon YM2[a]	–	80–90	[52]
PES[a]	–	83	[53]
PES	Polyethylene glycol methacrylate	95	
Poly-aryl-ether ketone[a]	–	~90	[54]
PSf	TiO_2 (2 wt.%)	90	[55]
PES	ZrO_2 (5 wt.%)	97	[56]
PEI/PPSU	–	79	[57]
PES	$LiNO_3$ (0.5 wt.%)	85	[58]
PSf	B-cyclodextrin hyperbranched PEI	79	[59]
CAB	POFA (2.5 wt.%)	85	Present work

[a]Commercially procured membranes.

solution permeated through the composite membranes has been shown in Fig. 12(B). HA removal capacity of the prepared membranes has been compared with other reported membranes in Table 4.

5. Conclusion

POFA/CAB composite membranes were prepared in the current investigation in which the concentration of POFA was increased from 1 to 2.5 wt.%. POFA was suitably modified by reducing the particle size to meet the requirement of the current work. The enhancement in water uptake capacity and porosity proved increase in hydrophilicity upon POFA addition. It was concluded that, even though the membranes were hydrophilic, beyond 2 wt.%, blocking of membrane pores by POFA had a negative effect on the permeation and porosity. This was further confirmed by SEM analysis, where morphology changed significantly after 2 wt.% POFA addition. FRR was recorded maximum for CAB 2 membrane that was 87.6%. Even though the removal of HA was maximum for CAB 2.5 (85.78%), the permeation property of the membrane was not satisfactory. In conclusion, CAB 2 membrane was considered to have optimum and balanced performance.

Thus, in conclusion, the concept of using a waste material, to purify another contaminant was successfully carried out. The adsorption behavior of POFA may be utilized in the future to treat wastewater streams containing textile dyes or heavy metals. Reducing the dimensions of POFA to nanoscale or suitable chemical modification may further ensure higher removal of water contaminants. The use of such industrial wastes, which are potential environmental pollutants, to curb the water contamination is an attractive notion which may lead to a new revolution in the field of membrane fabrication process.

Acknowledgements

Authors thank Vision Group on Science & Technology, Government of Karnataka, India for the CESEM award.

References

[1] X.-L. Li, L.-P. Zhu, B.-K. Zhu, Y.-Y. Xu, High-flux and anti-fouling cellulose nanofiltration membranes prepared via phase inversion with ionic liquid as solvent, Sep. Purif. Technol. 83 (2011) 66–73.
[2] C. Xing, H. Wang, Q. Hu, F. Xu, X. Cao, J. You, Y. Li, Mechanical and thermal properties of eco-friendly poly(propylene carbonate)/cellulose acetate butyrate blends, Carbohydr. Polym. 92 (2013) 1921–1927.
[3] M.H. Asgarkhani, S.M. Mousavi, E. Saljoughi, Cellulose acetate butyrate membrane containing TiO_2 nanoparticle: Preparation, characterization and permeation study, Korean J. Chem. Eng. 30 (2013) 1819–1824.
[4] A.D. Sabde, M.K. Trivedi, V. Ramachandhran, M.S. Hanra, B.M. Misra, Casting and characterization of cellulose acetate butyrate based UF membranes, Desalination 114 (1997) 223–232.
[5] M. Safiuddin, M. Abdus Salam, M.Z. Jumaat, Utilization of palm oil fuel ash in concrete: A review, J. Civ. Eng. Manage. 17 (2011) 234–247.
[6] M. Safiuddin, M.Z. Jumaat, M.A. Salam, M.S. Islam, R. Hashim, Utilization of solid wastes in construction materials, Int. J. Phys. Sci. 5 (2010) 1952–1963.
[7] A.S.M.A. Awal, M.W. Hussin, The effectiveness of palm oil fuel ash in preventing expansion due to alkali-silica reaction, Cem. Concr. Compos. 19 (1997) 367–372.
[8] M. Ghiaci, A. Abbaspur, R. Kia, F. Seyedeyn-Azad, Equilibrium isotherm studies for the sorption of benzene, toluene, and phenol onto organo-zeolites and as-synthesized MCM-41, Sep. Purif. Technol. 40 (2004) 217–229.
[9] B. Bayat, Combined removal of zinc(II) and cadmium (II) from aqueous solutions by adsorption onto high-calcium Turkish fly ash, Water Air Soil Pollut. 136 (2002) 69–92.

[10] V. Chantawong, N.W. Harvey, V.N. Bashkin, Comparison of heavy metal adsorptions by Thai kaolin and ballclay, Water Air Soil Pollut. 148 (2003) 111–125.
[11] H.R. Pant, H.J. Kim, M.K. Joshi, B. Pant, C.H. Park, J.I. Kim, K.S. Hui, C.S. Kim, One-step fabrication of multifunctional composite polyurethane spider-web-like nanofibrous membrane for water purification, J. Hazard. Mater. 264 (2014) 25–33.
[12] L. Zhu, Y. Dong, L. Li, J. Liu, S.-J. You, Coal fly ash industrial waste recycling for fabrication of mullite-whisker-structured porous ceramic membrane supports, RSC Adv. 5 (2015) 11163–11174.
[13] L. Li, C. Hu, X. Dai, W. Jin, C. Hu, F. Ma, The performance of a biological aerated filter loaded with a novel non-sintered fly-ash ceramsite as pretreatment for dual membrane processes, Environ. Technol. 36 (2015) 2024–2034.
[14] S. Kara, C. Aydiner, E. Demirbas, M. Kobya, N. Dizge, Modeling the effects of adsorbent dose and particle size on the adsorption of reactive textile dyes by fly ash, Desalination 212 (2007) 282–293.
[15] M. Ahmaruzzaman, V.K. Gupta, Rice husk and its ash as low-cost adsorbents in water and wastewater treatment, Ind. Eng. Chem. Res. 50 (2011) 13589–13613.
[16] U.R. Lakshmi, V.C. Srivastava, I.D. Mall, D.H. Lataye, Rice husk ash as an effective adsorbent: Evaluation of adsorptive characteristics for Indigo Carmine dye, J. Environ. Manage. 90 (2009) 710–720.
[17] L. Krishnamoorthy, P.M. Arif, R. Ahmedkhan, Separation of proteins from aqueous solution using cellulose acetate/poly(vinyl chloride) blend ultrafiltration membrane, J. Mater. Sci. 46 (2010) 2914–2921.
[18] V. Gupta, S. Sharma, I. Yadav, D. Mohan, Utilization of bagasse fly ash generated in the sugar industry for the removal and recovery of phenol and p-nitrophenol from wastewater, J. Chem. Technol. Biotechnol. 71 (1998) 180–186.
[19] V.K. Gupta, D. Mohan, S. Sharma, M. Sharma, Removal of basic dyes (Rhodamine B and methylene blue) from aqueous solutions using bagasse fly ash, Sep. Sci. Technol. 35 (2000) 2097–2113.
[20] E. Yildiz, Phosphate removal from water by fly ash using crossflow microfiltration, Sep. Purif. Technol. 35 (2004) 241–252.
[21] P.S. Saud, B. Pant, M. Park, S.-H. Chae, S.-J. Park, M. EI-Newehy, S.S. Al-Deyab, H.-Y. Kim, Preparation and photocatalytic activity of fly ash incorporated TiO_2 nanofibers for effective removal of organic pollutants, Ceram. Int. 41 (2015) 1771–1777.
[22] K.H. Chu, M.A. Hashim, Adsorption characteristics of trivalent chromium on palm oil fuel ash, Clean Technol. Environ. Policy 4 (2002) 8–15.
[23] M. Hasan, A.L. Ahmad, B.H. Hameed, Adsorption of reactive dye onto cross-linked chitosan/oil palm ash composite beads, Chem. Eng. J. 136 (2008) 164–172.
[24] S. Deng, R.B. Bai, Aminated polyacrylonitrile fibers for humic acid adsorption: Behaviors and mechanisms, Environ. Sci. Technol. 37 (2003) 5799–5805.
[25] H. Sehaqui, U. Perez de Larraya, P. Tingaut, T. Zimmermann, Humic acid adsorption onto cationic cellulose nanofibers for bioinspired removal of copper (II) and a positively charged dye, Soft Matter 11 (2015) 5294–5300.
[26] S. Wang, Q. Ma, Z.H. Zhu, Characteristics of unburned carbons and their application for humic acid removal from water, Fuel Process. Technol. 90 (2009) 375–380.
[27] T. Hartono, S. Wang, Q. Ma, Z. Zhu, Layer structured graphite oxide as a novel adsorbent for humic acid removal from aqueous solution, J. Colloid Interface Sci. 333 (2009) 114–119.
[28] J. Wang, L. Bi, Y. Ji, H. Ma, X. Yin, Removal of humic acid from aqueous solution by magnetically separable polyaniline: Adsorption behavior and mechanism, J. Colloid Interface Sci. 430 (2014) 140–146.
[29] A. Mehrparvar, A. Rahimpour, M. Jahanshahi, Modified ultrafiltration membranes for humic acid removal, J. Taiwan Inst. Chem. Eng. 45 (2014) 275–282.
[30] R.S. Hebbar, A.M. Isloor, A.F. Ismail, S.J. Shilton, A. Obaid, H.-K. Fun, Probing the morphology and anti-organic fouling behaviour of a polyetherimide membrane modified with hydrophilic organic acids as additives, New J. Chem. 39 (2015) 6141–6150.
[31] A. Sotto, A. Boromand, S. Balta, J. Kim, B. Van der Bruggen, Doping of polyethersulfone nanofiltration membranes: Antifouling effect observed at ultralow concentrations of TiO_2 nanoparticles, J. Mater. Chem. 21 (2011) 10311–10320.
[32] Z. Chen, M. Deng, Y. Chen, G. He, M. Wu, J. Wang, Preparation and performance of cellulose acetate/polyethyleneimine blend microfiltration membranes and their applications, J. Membr. Sci. 235 (2004) 73–86.
[33] V. Vatanpour, S.S. Madaeni, A.R. Khataee, E. Salehi, S. Zinadini, H.A. Monfared, TiO_2 embedded mixed matrix PES nanocomposite membranes: Influence of different sizes and types of nanoparticles on antifouling and performance, Desalination 292 (2012) 19–29.
[34] V. Vatanpour, S.S. Madaeni, R. Moradian, S. Zinadini, B. Astinchap, Novel antibifouling nanofiltration polyethersulfone membrane fabricated from embedding TiO_2 coated multiwalled carbon nanotubes, Sep. Purif. Technol. 90 (2012) 69–82.
[35] N.M. Altwair, M.M. Johari, S.F.S. Hashim, Strength activity index and microstructural characteristics of treated palm oil fuel ash, Int. J. Civ. Environ. Eng. 11 (2011) 100–107.
[36] A. Sharma, K. Srivastava, V. Devra, A. Rani, Modification in properties of fly ash through mechanical and chemical activation, Am. Chem. Sci. J. 2 (2012) 177–187.
[37] A. Sharma, S. Katara, S. Kabra, A. Rani, Acid activated fly ash, as a novel solid acid catalyst for esterification of acetic acid, Indian J. Appl. Res. 3 (2013) 37–39.
[38] K.Y. Foo, B.H. Hameed, Utilization of rice husk ash as novel adsorbent: A judicious recycling of the colloidal agricultural waste, Adv. Colloid Interface Sci. 152 (2009) 39–47.
[39] D.C.D. Nath, S. Bandyopadhyay, A. Yu, D. Blackburn, C. White, High strength bio-composite films of poly (vinyl alcohol) reinforced with chemically modified-fly ash, J. Mater. Sci. 45 (2009) 1354–1360.
[40] H. Wu, J. Mansouri, V. Chen, Silica nanoparticles as carriers of antifouling ligands for PVDF ultrafiltration membranes, J. Membr. Sci. 433 (2013) 135–151.
[41] V.R. Pereira, A.M. Isloor, A. Ahmed, A. Ismail, Preparation, characterization and the effect of PANI coated

TiO_2 nanocomposites on the performance of polysulfone ultrafiltration membranes, New J. Chem. 39 (2015) 703–712.
[42] S. Qiu, L. Wu, X. Pan, L. Zhang, H. Chen, C. Gao, Preparation and properties of functionalized carbon nanotube/PSF blend ultrafiltration membranes, J. Membr. Sci. 342 (2009) 165–172.
[43] S. Zhao, Z. Wang, X. Wei, X. Tian, J. Wang, S. Yang, S. Wang, Comparison study of the effect of PVP and PANI nanofibers additives on membrane formation mechanism, structure and performance, J. Membr. Sci. 385–386 (2011) 110–122.
[44] S. Xia, M. Ni, Preparation of poly(vinylidene fluoride) membranes with graphene oxide addition for natural organic matter removal, J. Membr. Sci. 473 (2015) 54–62.
[45] J. Hong, Y. He, Effects of nano sized zinc oxide on the performance of PVDF microfiltration membranes, Desalination 302 (2012) 71–79.
[46] A. Cui, Z. Liu, C. Xiao, Y. Zhang, Effect of micro-sized SiO_2-particle on the performance of PVDF blend membranes via TIPS, J. Membr. Sci. 360 (2010) 259–264.
[47] F. Liu, N.A. Hashim, Y. Liu, M.R.M. Abed, K. Li, Progress in the production and modification of PVDF membranes, J. Membr. Sci. 375 (2011) 1–27.
[48] M. Hashino, K. Hirami, T. Katagiri, N. Kubota, Y. Ohmukai, T. Ishigami, T. Maruyama, H. Matsuyama, Effects of three natural organic matter types on cellulose acetate butyrate microfiltration membrane fouling, J. Membr. Sci. 379 (2011) 233–238.
[49] P.S. Yune, J.E. Kilduff, G. Belfort, Fouling-resistant properties of a surface-modified poly(ether sulfone) ultrafiltration membrane grafted with poly(ethylene glycol)-amide binary monomers, J. Membr. Sci. 377 (2011) 159–166.
[50] D.C.D. Nath, S. Bandyopadhyay, P. Boughton, A. Yu, D. Blackburn, C. White, Chemically modified fly ash for fabricating super-strong biodegradable poly(vinyl alcohol) composite films, J. Mater. Sci. 45 (2010) 2625–2632.
[51] A. Alpatova, S. Verbych, M. Bryk, R. Nigmatullin, N. Hilal, Ultrafiltration of water containing natural organic matter: Heavy metal removing in the hybrid complexation–ultrafiltration process, Sep. Purif. Technol. 40 (2004) 155–162.
[52] I.L. Küchler, N. Miekeley, Ultrafiltration of humic compounds through low molecular mass cut-off level membranes, Sci. Total Environ. 154 (1994) 23–28.
[53] P.D. Peeva, A.E. Palupi, M. Ulbricht, Ultrafiltration of humic acid solutions through unmodified and surface functionalized low-fouling polyethersulfone membranes—Effects of feed properties, molecular weight cut-off and membrane chemistry on fouling behavior and cleanability, Sep. Purif. Technol. 81 (2011) 124–133.
[54] Z. Domany, I. Galambos, G. Vatai, E. Bekassy-Molnar, Humic substances removal from drinking water by membrane filtration, Desalination 145 (2002) 333–337.
[55] N.A.A. Hamid, A.F. Ismail, T. Matsuura, A.W. Zularisam, W.J. Lau, E. Yuliwati, M.S. Abdullah, Morphological and separation performance study of polysulfone/titanium dioxide (PSF/TiO_2) ultrafiltration membranes for humic acid removal, Desalination 273 (2011) 85–92.
[56] Y.L. Thuyavan, N. Anantharaman, G. Arthanareeswaran, A.F. Ismail, Adsorptive removal of humic acid by zirconia embedded in a poly(ether sulfone) membrane, Ind. Eng. Chem. Res. 53 (2014) 11355–11364.
[57] L.-L. Hwang, H.-H. Tseng, J.-C. Chen, Fabrication of polyphenylsulfone/polyetherimide blend membranes for ultrafiltration applications: The effects of blending ratio on membrane properties and humic acid removal performance, J. Membr. Sci. 384 (2011) 72–81.
[58] J.-J. Qin, M.H. Oo, Y. Li, Hollow fiber ultrafiltration membranes with enhanced flux for humic acid removal, J. Membr. Sci. 247 (2005) 119–125.
[59] S.P. Malinga, O.A. Arotiba, R.W.M. Krause, S.F. Mapolie, M.S. Diallo, B.B. Mamba, Nanostructured β-cyclodextrin-hyperbranched polyethyleneimine (β-CD-HPEI) embedded in polysulfone membrane for the removal of humic acid from water, Sep. Sci. Technol. 48 (2013) 2724–2734.